Control of a Digital Micromirror Device Using the Bang-Bang Technique

Hassen M. Ouakad[†] and Abdelali El Aroudi[‡]

†Mechanical Engineering Department, King Fahd University of Petroleum and Minerals, Dhahran, Saudi Arabia
Email: houakad@kfupm.edu.sa
‡Dept. of Electrical Engineering, Electronics and Automatic Control, Universitat Rovira i Virgili, Tarragona, Spain
Email: abdelali.elaroudi@urv.cat

Abstract– In this study, a control strategy is applied to a Digital Micromirror Device (DMD) to maneuver its angular motion. The micromirror is actuated using an electrostatic field. The equations of motion of the system are derived using the Extended Hamilton's Principle. The static response of the DMD for different DC loads (bias and address voltages) is analyzed. The linear vibration behavior of the DMD is examined by plotting the natural frequencies versus the considered DC voltages. The proposed control strategy is done by the Bang-Bang technique which is suitable in optimal control problems where the control switches from one extreme to the other at certain time instants. This control strategy allowed decreasing the residual vibration of the micromirror when it switches from a position to another and then reduced its resultant switching time.

1. Introduction

In the few recent years, there has been major focus on controlling microelectromechanical systems (MEMS) especially those used in the light processing devices. In fact, now there is a new MEMS-based projection display technology called Digital Light Processing (DLP) that accepts digital video and transmits to the eye a burst of digital light pulses that the eye interprets as a color analog image [1,2]. DLP is based on a MEMS device known as the Digital Micromirror Device (DMD). Previous studies introduced several methods for the modeling of micromirrors [3-7]. For example, Chaabane et al [7] developed a continuous model that couples the bending and angular motions. The resulting ROM consists of two coupled ordinary-differential equations that represent the first modes of vibration associated with bending and torsion. The current study is a continuation of the work by Chaabane et al [7] and focuses on the control of the Micromirror to maneuver its angular motion by using the Bang-Bang control technique. This remaining of the paper is organized as follows: In the first part, the modelling and dynamics of the DMD developed by Chaabane et al [7] are reviewed using Lagrange's equations. In the second part, we will examine the static and dynamic behavior of the micromirror. In the third part, the Bang-Bang technique is proposed to control the angular motion of the DMD.

2. Problem formulation and system modeling

The DMD system under consideration is composed of two flexible hinges, a rigid yoke, a rigid post, a rigid mirror, four landing spring tips, and four addressing electrodes, Fig. 1. The hinges are modeled by two microbeams, each of length l, width w, and thickness h. These beams are fixed from one side and connected to a rigid H-shaped plate of length L_y, thickness h_y, and width w_2, representing the yoke, on the other side. On top of the yoke sets a rigid square perforated bar of length L_p, internal and external lengths respectively, c_1 and c_2 which model the post. Above this bar sets a rigid squared plate (the micromirror) of length L_m and thickness h_m. The spring tips are modeled by four linear translational springs of undeformed length l_0 and equivalent stiffness k determined from the assumption that the spring tips deflect in their first mode of vibration. In addition, it is assumed that the sliding friction of the spring tips against the substrate is negligible. Beneath the micromirror set two rectangular electrodes each of length e_m and width b_2-b_1, where b_1 denotes the distance between the x-axis and the inner micromirror electrodes' edge and b_2 represents the distance between the x-axis and the outer micromirror electrodes' edge. Two reinforcing rectangular electrodes set under the yoke; each of length e_y and width a_2-a_1, where a_1 is the distance between the x-axis and the inner yoke electrodes' edge and a_2 is the distance between the x-axis and the outer yoke electrodes' edge. The yoke addressing electrodes are at the lower height level (substrate), whereas the micromirror addressing electrodes are at the same height level as the yoke. Then, the air gap between the micromirror and its electrodes is L_p and the air gap between the yoke and its electrodes is denoted by H.
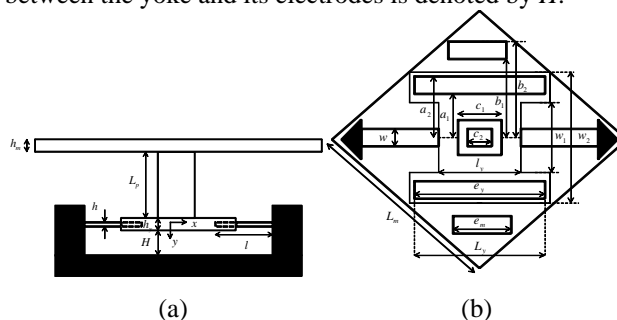

(a)   (b)

Fig. 1: Schematic of the micromirror device: (a) side view, (b) top view.

A reduced-order model can be deduced by approximating the hinges by linear translational and torsional springs associated with bending and torsion, respectively. The numerical values of the model parameters are listed in Table 1.

Table 1: The micromirror geometrical and material parameters.

ρ	2.7 g/cm^3	L_m	16 µm	w	0.78 µm	b_2	9 µm
E	69 GPa	h_m	0.5 µm	w_1	3.6 ìm µm	l_s	2.58 µm
v	0.33	H	1.3 µm	w_2	9.2 µm	w_s	0.65 µm
G	25.94 GPa	e_y	9.2 µm	L_y	9.4 µm	h_s	0.1 µm
ε_0	$\frac{1}{36\pi10^9}$	e_m	5 µm	l_y	5.2 µm	c_1	3.7 µm
g	9.81 m/s^2	a_1	1.9 µm	h_y	0.5 µm	c_2	3.2 µm
h	0.1 µm	a_2	4.5 µm	L_p	2.5 µm	Q	10
l	3.9 µm	b_1	6 µm				

The micromirror can be driven to rotate in one direction by supplying a voltage V to the corresponding side electrodes. This results in an electrostatic potential between the electrodes and the upper structure (yoke – micromirror). The resulting electrostatic potential generates two electrostatic pressures P_m and P_y on the surfaces of the yoke and the micromirror respectively, which in return produce an electrostatic force F_m+F_y, and hence an electrostatic moment M_m+M_y around the suspension point. Subscripts m and y refer to the micromirror and the yoke, respectively. In response to these electrostatic forces, the rigid yoke–post–micromirror struture tends to rotate at an angle θ_y and bend down a distance u_y simultaneously. Among the three possible configurations proposed in [7], two are adopted:

- Configuration 1: no contact between the springs and the landing area;

- Configuration 2: contact of two springs with one side of the landing area (one side contact).

The motion can be described by one of two sets of equations associated with the above configurations. The DMD motion can switch between the above configurations. The equations of motion are derived from the kinetic and potential energies of the DMD using Lagrange's equations applied to discrete systems:

$$\frac{\partial}{\partial t}\left(\frac{\partial L}{\partial \dot{q}_i}\right)-\frac{\partial L}{\partial q_i}=0, \qquad (18)$$

where $L = K_{total} - V_{total}$, K_{total} and V_{total} represents the kinetic and the potential energy respectively and q_i represents the displacement associated with every degree of freedom (torsion and bending).

$$q_1 = \theta_y, \; q_2 = u_y \qquad (20)$$

✓ *First configuration*

We obtain the following set of equations:

$$\begin{cases} J\theta_y'' + \left(-\frac{\alpha g}{2}+\frac{2GJ_p}{l}\right)\theta_y + \frac{\alpha}{2}u_y''\theta_y - \frac{V_1^2}{2}\frac{\partial C_{right}}{\partial \theta_y} - \frac{V_2^2}{2}\frac{\partial C_{left}}{\partial \theta_y} = 0 \\ Mu_y'' + \frac{\alpha}{2}\theta_y\theta_y'' + \frac{\alpha}{2}\theta_y'^2 + \frac{24E_0I_b}{l^3}u_y - gM - \frac{V_1^2}{2}\frac{\partial C_{right}}{\partial u_y} - \frac{V_2^2}{2}\frac{\partial C_{left}}{\partial u_y} = 0 \end{cases}$$
$$(21)$$

For convenience, we use the following nondimensional variables

$$\theta_y = \theta_{cr}\,\theta\,, \quad u_y = H\,u\,, \quad T = \tau.t\,, \qquad (24)$$

where θ_{cr} is the critical angular deflection and τ is the time constant defined as follows:

$$\theta_{cr} = \frac{2H}{w_2}, \quad \tau = \sqrt{\frac{J_{hinge}l^2}{GJ_p}} \qquad (25)$$

So the system in (21) becomes:

$$\begin{cases} \ddot{\theta} + \left(-\frac{\alpha g\tau^2}{2J}+\frac{2GJ_p\tau^2}{Jl}\right)\theta + \frac{H\alpha}{2J}\ddot{u}\theta = \frac{\tau^2V_1^2}{2J\theta_{cr}^2}\frac{\partial C_{right}}{\partial \theta} + \frac{\tau^2V_2^2}{2J\theta_{cr}^2}\frac{\partial C_{left}}{\partial \theta} \\ \ddot{u} + \frac{24E_0I_b\tau^2}{l^3M}u = \frac{g\tau^2}{H} - \frac{\alpha\theta_{cr}^2}{2HM}\theta\ddot{\theta} - \frac{\alpha\theta_{cr}^2}{2HM}\dot{\theta}^2 + \frac{V_1^2\tau^2}{2H^2M}\frac{\partial C_{right}}{\partial u} + \frac{V_2^2\tau^2}{2H^2M}\frac{\partial C_{left}}{\partial u} \end{cases}$$
$$(26)$$

✓ *Second configuration*

After applying the Lagrange's equations for the second configuration of the micromirror, and using (22)-(25) the equations of motion become

$$\begin{cases} \ddot{\theta} + \left(-\frac{\alpha g\tau^2}{2J}+\frac{2GJ_p\tau^2}{Jl}\right)\theta + \frac{H\alpha}{2J}\ddot{u}\theta + \frac{\tau^2k}{J}\left[\begin{array}{c}-l_0^2 2\theta\theta_{cr} + l_0\left(\frac{|\theta|}{\theta}w_2 - 2H\theta\theta_{cr}(-1+u)\right) + \\ \frac{1}{4}w_2\left(2\theta\theta_{cr}w_2 + 4H\frac{|\theta|}{\theta}(-1+u)\right)\end{array}\right] = \\ \qquad\qquad\qquad \frac{\tau^2V_1^2}{2J\theta_{cr}^2}\frac{\partial C_{right}}{\partial \theta} + \frac{\tau^2V_2^2}{2J\theta_{cr}^2}\frac{\partial C_{left}}{\partial \theta} \\ \ddot{u} + \frac{24E_0I_b\tau^2}{Ml^3}u + \frac{\alpha\theta_{cr}^2}{2HM}\dot{\theta}^2 + \frac{\alpha\theta_{cr}^2}{2HM}\theta\ddot{\theta} - \frac{g\tau^2}{H} + \frac{k}{HM}\tau^2\left(2H(u-1)+2l_0+w_2\theta_{cr}|\theta|\right) = \\ \qquad\qquad\qquad \frac{V_1^2\tau^2}{2H^2M}\frac{\partial C_{right}}{\partial u} + \frac{V_2^2\tau^2}{2H^2M}\frac{\partial C_{left}}{\partial u} \end{cases}$$
$$(27)$$

3. The static behaviour of the DMD

The static equations of the micromirror when subjected to step voltages for both the first and second configurations is obtained by setting the time in (26)-(27) equal to zero.

To solve numerically for the static positions of the micromirror's motion in the first configuration, first we assume V_2 zero and we increase V_1 value from 0 until getting instability (Pull-in). Figs 3 and 4 show the torsion static deflection and the bending one respectively in term of V_1 for $V_2=0$ for both the first and the second configurations. It can be concluded that as the voltage V_1 is increases, the system tends to reach pull-in instability.

When solving for the static positions for different V_2 voltages (Figs. 3 and 4), we conclude that as V_2 increases pull-in tilting angle decreases and pull-in downward bending increases for the first configuration: this seems to be expected since V_2 tends to increase attracting forces beneath the yoke and the mirror, thus, the

2

transverse deflection is more considerable. It can be also noticed from Figs. 3 and 4 that increasing V_1 for a constant values V_2 leads to move up the static position until instability occurs. On the other hand, increasing V_2, resulted in a decrease of the the pull-in tilting angle value, and an increase in the pull-in bending value.
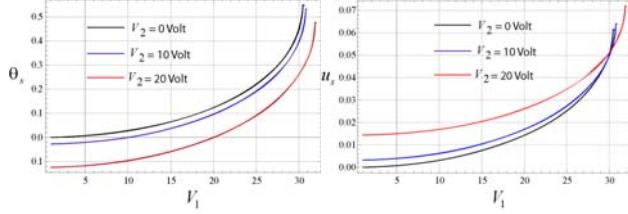

Fig. 3: Variation if the static torsion versus the applied voltage V_1 for the two configurations (for different values of V_2).
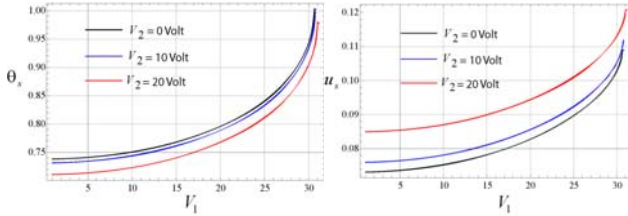

Fig. 4: Variation if the static bending versus the applied voltage V_1 for the two configurations (for different values of V_2).

4. The linear vibration problem

The major point of this section is the dynamic analysis of linear vibrations of the DMD for different DC voltages using the obtained model. The natural frequencies, for the torsion and the bending, are determined while varying the voltages V_1 and V_2 for the first configuration. Figure 5 shows the variation of the first natural frequencies for both the torsion and the bending motion of the DMD. We can conclude that increasing the applied DC voltage V_1 yields a drop in both natural frequencies and finally the pull-in instability is reached. The first natural frequency of torsion goes to zero at pull-in and that of the bending one undergoes significant reductions.
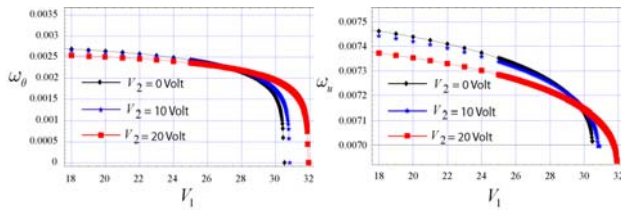

Fig. 5: Variation if the natural frequency with the applied voltage V_1 for the torsion and bending motion (for different values of V_2).

5. Control of the DMD vibration

In this section, we will derive all the instant of times that will specify the overall mechanical switching response of the DMD system. In our model, we consider two parameters: The first one is the switching voltage and the second is the switching time needed to switch between the

two previously presented configurations in Section 2.2.2. For the switching voltage, we will consider V_1 as maximum at all times and V_2 as maximum at all times. This procedure is known as the Bang-Bang method. For instance, we will consider a passage between the first configuration, and then the second one and finally we return to the first configuration. We are summarizing this in the following diagram:

$$\begin{cases} t \leq 0 & We \quad have \quad X0 = \begin{bmatrix} 0 \\ -10 \end{bmatrix} & \begin{cases} V_1 = V_{1\max} & 1^{st} Conf \\ V_2 = V_{21\max} \end{cases} \\ 0 \leq t \leq ts & We \quad have \quad X1 = \begin{bmatrix} \theta_{d1} \\ u_{d1} \end{bmatrix} & \begin{cases} V_1 = -V_{1\max} & 1^{st} Conf \\ V_2 = V_{21\max} \end{cases} \\ ts \leq t \leq t1 & We \quad have \quad X2 = \begin{bmatrix} \theta_{d2} \\ u_{d2} \end{bmatrix} & \begin{cases} V_1 = V_{1\max} & 1^{st} Conf \\ V_2 = V_{22\max} \end{cases} \\ t1 \leq t \leq t2 & We \quad have \quad X3 = \begin{bmatrix} \theta_{d3} \\ u_{d3} \end{bmatrix} & \begin{cases} V_1 = V_{1\max} & 2^{nd} Conf \\ V_2 = V_{22\max} \end{cases} \\ t2 \leq t \leq t3 & We \quad have \quad X4 = \begin{bmatrix} \theta_{d4} \\ u_{d4} \end{bmatrix} & \begin{cases} V_1 = V_{1\max} & 1^{st} Conf \\ V_2 = V_{21\max} \end{cases} \\ t3 \leq t \leq \infty & We \quad have \quad X5 = \begin{bmatrix} \theta_{d5} \\ u_{d5} \end{bmatrix} & \begin{cases} V_1 = V_{1\max} & 1^{st} Conf \\ V_2 = V_{21\max} \end{cases} \end{cases}$$

As we can notice, we have here four unknowns to solve for> We hence consider four conditions which are:

$$\begin{cases} \left.\frac{\partial X1(1)}{\partial t}\right|_{t=t_s} ; & X2|_{t=t_1} = X3|_{t=t_1} ; & X3|_{t=t_2} = X4|_{t=t_2} ; & X4|_{t=t_3} = X5|_{t=t_3} \end{cases}$$

In optimal control problems, it is sometimes the case that a control is restricted to be between a lower and an upper bound. If the optimal control switches from one extreme to the other at certain times (i.e. is never strictly in between the bounds) then the control is referred to as a Bang-Bang control or a Bang-Bang solution.

Bang-Bang controls frequently arise in minimum time problems. For example if it is desired to stop a car in the shortest possible time after a traffic light turns red, the solution is to apply maximum braking as soon as the light changes. This solution (a rather uncomfortable one for the passengers) is a Bang-Bang solution: no braking followed by maximum braking. Such solutions also arise when the Hamiltonian is linear in the control variable; application of Pontryagin's minimum principle will then lead to pushing the control to its upper or lower bound depending on the sign of the coefficient of u in the Hamiltonian.

A primitive type of feedback Bang-Bang control technique that is used in systems that are slow and/or poorly designed. It consists of the following logic:

- ✓ If the output is less than your target, then go full forward;
- ✓ If the output is greater than your target, then either go full reverse turn off;
- ✓ If we do this, the system is sometimes called an on-off control system.

There are three major problems with this method:
- ✓ It is extremely unstable. If you have any significant delay introduced in your feedback step, you are going

3

to see an unpleasant oscillation around the target value that will never peter out.

- ✓ It is noisy. It was called 'bang-bang' control due to the noise that it made in mechanical implementations of the system. In electronic methods, it can cause power surges and ringing in the circuit as the control switches on and off.
- ✓ It is not ergonomic. Most humans like to have some steady acceleration with a minimization of jerk.

Bang-Bang control is commonly found in old refrigeration and air conditioning systems. It is also found in programs written by otherwise knowledgeable coders who think they can solve the mechanical and electronic problems raised by this method in software. Slightly less clueless programmers will use proportional control. More clever ones will use PD control, PID control, or fuzzy logic.

Applying a step voltage to the system drives the Micromirror through a set of vibrations around the static positions. To evaluate the accuracy of the 2nd order nonlinear approximate solution, we use MATHEMATICA to compute a numerical solution for the system defined by the 2 nonlinear equations of motion described in the previous chapter. The applied step voltage is illustrated in Fig. 6. To obtained DMD tilting angle function after applying the step voltage is shown in Fig. 7.
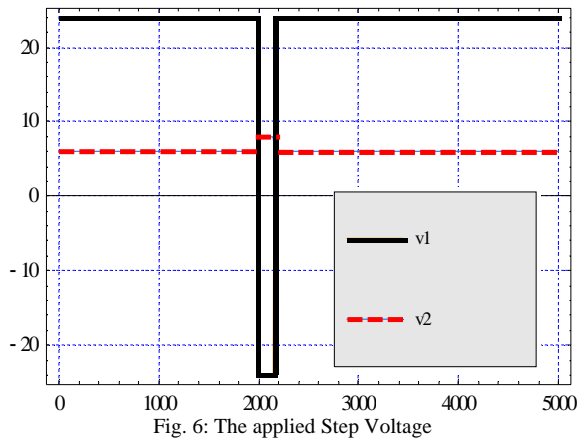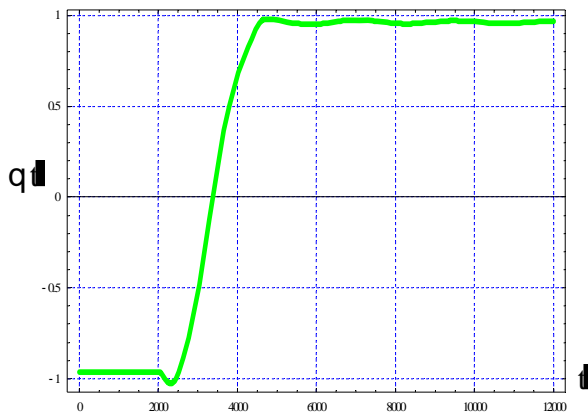

Fig. 6: The applied Step Voltage

Fig. 7: The response of the system to the applied step voltage

We finally compare in Fig. 8 the obtained controlled response with the one provided by TI in the literature.
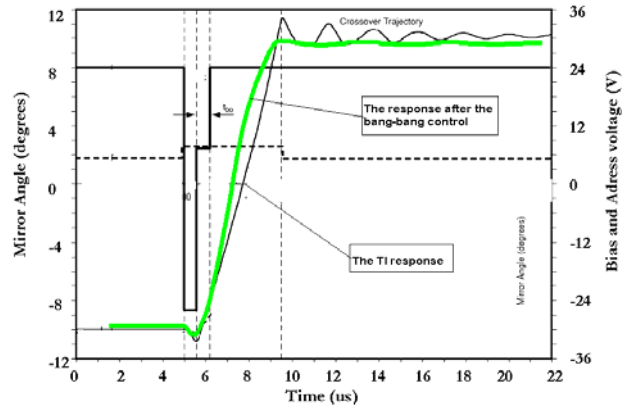

Fig. 8: The Bang-Bang response versus the TI response.

6. Conclusion

In this work, we considered the control of the DMD angular motion using Bang-Bang technique. The design of the control was based on a model formed of two ordinary differential equations which couple the bending and torsion motions of the micromirror. This work is applicable to drive the DMD device to angles below pull-in threshold. Current research focuses on the control robustness against parameters uncertainties and internal disturbances. In particular, the ZVD shaper done by Chaabane et al [7] and other shaping techniques will be applied to satisfy certain criteria with regard to system performance including control robustness.

References

[1] L.J. Hornbeck, "Digital Light Processing: A New MEMS-Based Display Technology", Texas Instruments report, pp 1-24, 1989.
[2] L. Yoder, "An Introduction to the Digital Light Processing (DLP™) Technology", Texas Instruments report, pp 1-8, 1995.
[3] C. Lee, "Design and fabrication of epitaxial silicon micromirror devices", Sensors and Actuators A, pp 115, 2004.
[4] Y. Yao, X. Zhang, G. Wang, and L. Huang, "Efficient Modeling of a Biaxial Micromirror with Decoupled Mechanism", Sensors and Actuators A, Vol. 120, pp. 7–16, 2005.
[5] J. M. Huang, A.Q. Liu, Z. L. Deng, Q.X. Zhang , J. Ahn, and A. Asundi. "An approach to the coupling effect between torsion and bending for electrostatic torsional micromirrors", Sensors and Actuators A, Vol. 115, pp. 159–167, 2004.
[6] J. P. Zhao, H. L. Chen, J. Ming Huang, A. Q. Liu, "A Study of Dynamic Characteristics and Simulation of MEMS Torsional Micromirrors", Sensors and Actuators A, Vol. 120, pp. 199–210, 2005.
[7] G. Chaabane, E. M. Abdel-Rahman, A. H. Nayfeh, S. Choura, S. El-Borgi and H. Jammoussi, "Dynamic Analysis of a Digital Micromirror Device", The ASME International Mechanical Engineering Congress & Exposition, Chicago, IL, USA, 2006.